THE ASTROPHYSICAL JOURNAL, 444:L49–L52, 1995 May 1

# EXTREME NITROGEN ENRICHMENT IN THE ASYMMETRICAL PLANETARY NEBULA M1-75

MARTÍN A. GUERRERO
Instituto de Astrofisica de Canarias, E-38200 La Laguna (Tenerife), Spain; mar@iac.es
LETIZIA STANGHELLINI
Osservatorio Astronomico di Bologna, via Zamboni 33, I-40126 Bologna, Italy
AND
ARTURO MANCHADO
Instituto de Astrofisica de Canarias, E-38200 La Laguna (Tenerife), Spain
*Received 1995 January 10; accepted 1995 February 9*

## ABSTRACT

In the framework of the morphological survey of northern sky planetary nebulae, in progress at the IAC, we investigate in detail those nebulae that show peculiarities or that have not been studied before. By means of narrowband imaging and accurate two-dimensional spectroscopy we analyzed the peculiar nebula M1-75. Its morphology is very complex, consisting of two contiguous shells, surrounded by two previously undetected fainter lobes. Detailed plasma analysis showed an extreme nitrogen enrichment in the outermost shell (N/O = 2.85), as well as a high helium abundance (He/H = 0.18), making this object a good candidate for peculiar stellar evolutionary paths. The detected abundances of heavy elements are among the highest ever detected in a galactic planetary nebula.

*Subject headings:* planetary nebulae: individual (M1-75) — stars: evolution

## 1. INTRODUCTION

The correspondence between the chemical and morphological characteristics of planetary nebulae (PNs) was demonstrated by Peimbert (1978), who defined Types I and II PNs on the basis of their nitrogen and helium enrichment. In order to build a constructive framework to compare observations and theory, additional investigation is in order presently. In particular, the widening of homogeneous databases of galactic and extragalactic PNs improves the field in a statistical sense. Stanghellini, Corradi, & Schwarz (1993) used the survey of southern PN images (Schwarz, Corradi, & Melnick 1992) to study the correlations between nebular two-dimensional shapes, and the evolutionary stages and the masses of the central stars. More recently, Manchado et al. (1995) started a survey of northern PNs via narrowband imagery.

Among the peculiar nebulae disclosed by Manchado et al.'s survey is M1-75. According to the morphological classification scheme given by Stanghellini et al. (1993), this is an irregular nebula with a multiple/irregular shell structure with detached lobes (or ringlets). We derive the information from narrowband imagery and from differential spectroscopy.

## 2. OBSERVATIONS

We observed M1-75 through two narrowband filters: H$\alpha$ + [N II] (FWHM 100 Å) and [O III] $\lambda$5007 (FWHM 30 Å), using the 0.8 m IAC 80 telescope at the Observatorio del Teide (Tenerife) in 1994 January. We used a 1024 × 1024 Thomson CCD with pixel-size of 20 $\mu$m. Four images of M1-75 were taken at each filter, each lasting 15 minutes. These images were added to obtain the final pictures of Figure 1 (Plate L1). The pixel size is 0".435 with a field of view 7'.4. The seeing was less than or equal to 1".5 throughout the observations.

The spectral data were collected at the Isaac Newton Telescope (Observatorio del Roque de los Muchachos, La Palma) in 1994 May, using the IDS (Intermediate Dispersion Spectrograph) (Unger et al. 1988) with the 235 mm camera. The 300 l mm$^{-1}$ grating R300V gave a dispersion of 3.12 Å pixel$^{-1}$, covering a spectral range from 3600 to 7200 Å. Spectral resolution was 6.5 Å. We used a long slit along the principal axes of elongation. A second slit was placed 90° from the first. We observed along the first slit with two exposures of 30 minutes each, and along the perpendicular slit with one 30 minute exposure. Slit positions with respect to the nebula are presented in Figure 1.

## 3. SPECTRAL ANALYSIS

The two-dimensional spectra were cut so that one-dimensional spectra could be obtained for each different region of the nebula. To show more precisely where the spectra were extracted, we present in Figure 2 the surface brightness profile of the [N II] $\lambda$6584 line, extracted from the low-dispersion spectrum at the principal position angle. In Figure 2 we can single out three different zones within M1-75: zone A corresponds to the central region; zone B is a second, attached, irregular shell of higher emission in the light of [N II]; and zone C comprises the faint, extended, and asymmetrical ringlets (or lobes) about the shells. From Figure 2 we see that the flux does not fall to zero between zones B and C. Thus the outer structures are probably two-dimensional projections of very thin shells or filaments, rather than rings. On the secondary slit position, only zones A and B were detected, as can be inferred from Figure 1. The final one-dimensional spectrum of region C is simply cut from the relative region of the first slit position, whereas the final spectra for zones A and B are obtained by adding these zone contributions from the two slit positions. Figure 3 shows the one-dimensional spectra for zones A, B, and C, respectively. There is a scarcity of nebular lines in zone C. No stellar continuum has been detected.

The optical extinction constant was determined by fitting the observed Balmer decrement (H$\alpha$, H$\beta$, and H$\gamma$ lines) in region B, since its spectrum have the highest signal-to-noise ratio, to the theoretical Balmer lines ratios (Brocklehurst 1971)

1995ApJ...444L..49G

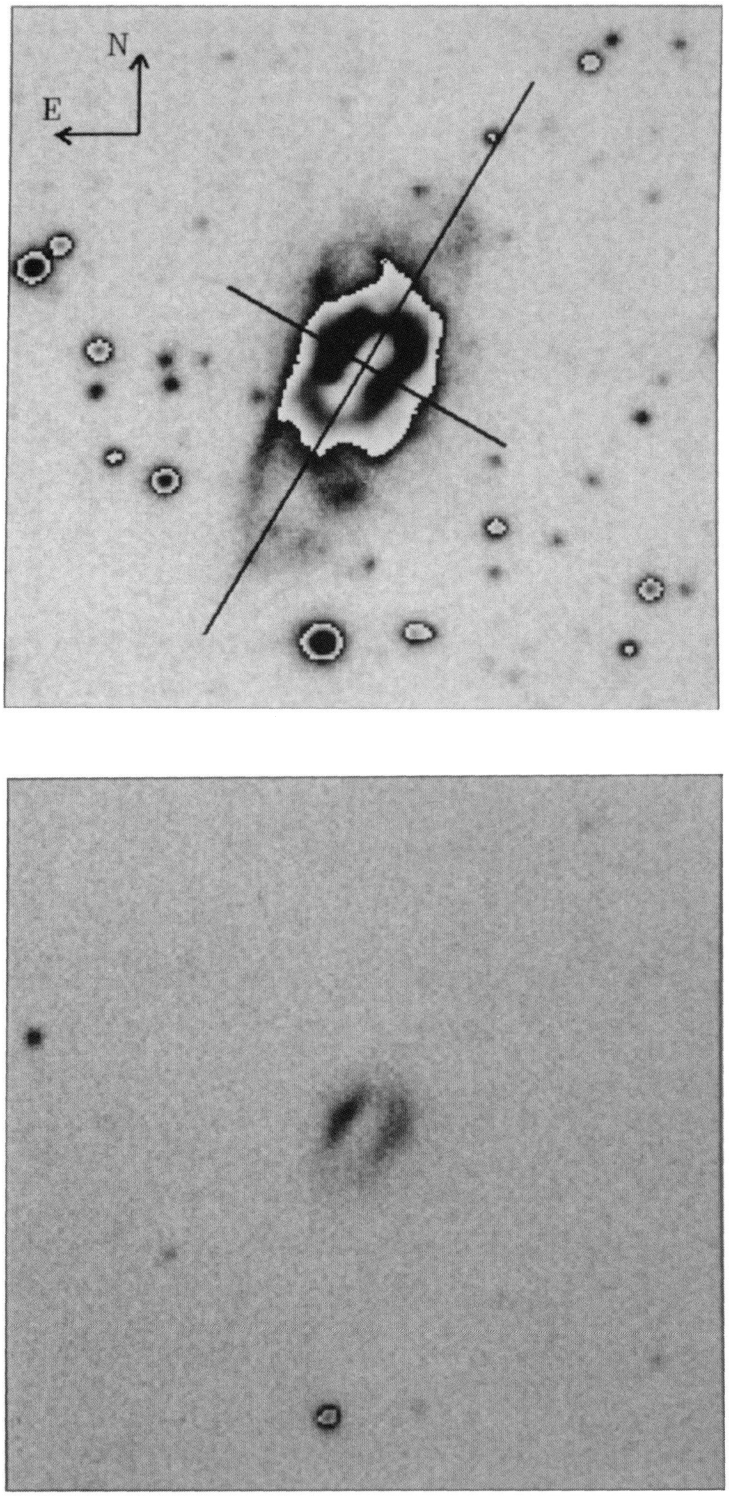

FIG. 1.—(*Top*) $H\alpha$ + [N II] image of M1-75. The picture has been displayed at two levels of intensity to show both the bright and faint features. The slit positions of low-resolution spectra are shown. (*Bottom*) [O III] image of M1-75. In both filters, the field of view is 104″.

GUERRERO, STANGHELLINI, & MANCHADO (see 444, L49)

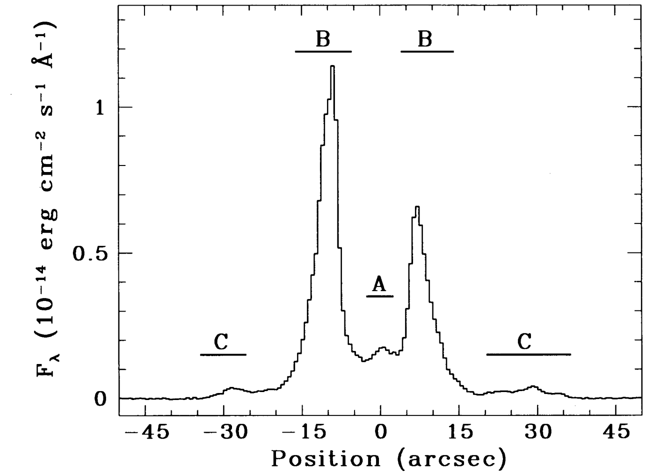

FIG. 2.—Surface brightness profile of the [N II] $\lambda 6584$ line extracted from the low-dispersion spectra along the major elongation axis.

adopting case B recombination ($T_e = 10^4$ K and $N_e = 10^4$ cm$^{-3}$). Taking into account the errors involved in the flux measurement of the Balmer lines, we adopted $c_\beta = 2.3 \pm 0.1$, which is in good agreement with the value $c_\beta = 2.4$ given by Aller & Keyes (1987). The observed line fluxes were dereddened using the reddening function, $f(\lambda)$, derived from the normal extinction law (Whitford 1958). Although a slightly lower value for the extinction is deduced from the H$\alpha$/H$\beta$ ratio in region A, we used the same value as in region B, because line flux measurements in the central region are more uncertain. In Table 1 we list the observed and dereddened relative intensities of the nebular lines corresponding to the spectra of Figure 3. All intensities are scaled to $I_{\mathrm{H}\beta} = 100$, except those of region C where no H$\beta$ flux was detected and intensities are scaled to $I_{\mathrm{H}\alpha} = 100$.

Ionic abundances were calculated for the three zones via the five-level atom program provided by Preite-Martinez (1986). The calculation of the physical conditions in zones A and C was not possible (see Table 2). Low-excitation ionic abundances were calculated with the [N II] electron temperatures, while high-excitation lines were treated with the [O III] one. Column (1) gives the diagnostic, whiles columns (2) and (3) give the values for that diagnostic in the A and B zones. In region C, it was not possible to calculate the electron density and temperature, due to the weakness of the diagnostic lines. However, assuming the same electronic temperature than in region B and an electronic density of 100 cm$^{-3}$, it was possible to derive a value of $6 \times 10^{-4}$ for the N$^+$/H$^+$ abundance. Even if all the nitrogen was in this ionization state (N$^+$), the nitrogen abundances will be 6 times higher than the solar value. The ionic and elemental abundances, derived on the basis of the standard ionization correction factors, as well as their associated errors, are given at the end of Table 2. Errors were estimated taking into account the uncertainties associated with the line strength measurements and those due to the electron densities and temperature calculations. Helium abundances were calculated

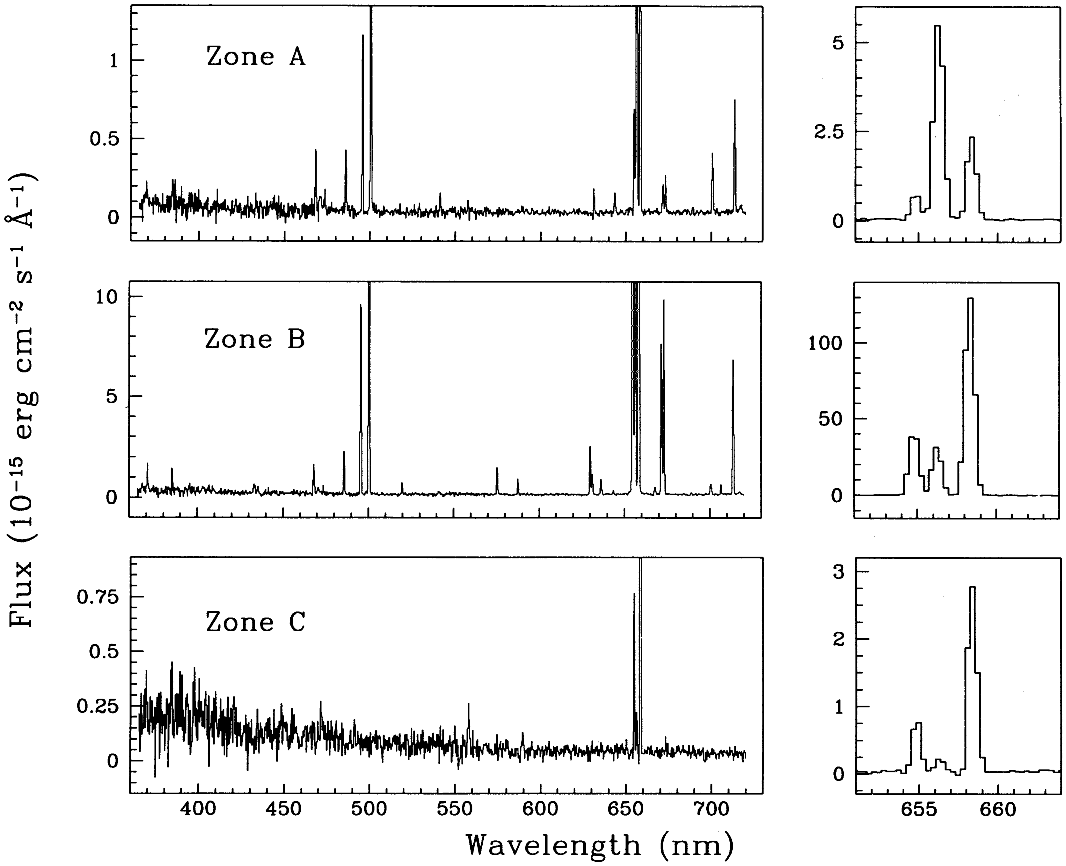

FIG. 3.—One-dimensional spectra of M1-75 (*top*) zone A, (*center*) zone B, and (*bottom*) zone C. The H$\alpha$ and [N II] spectral region is shown at different scale in order to bring out the relation between these lines.

TABLE 1

Observed and Dereddened Line Intensity Ratios for M1-75

| Line | $f(\lambda)$ | A $I_{obs}$ | A $I_{der}$ | B $I_{obs}$ | B $I_{der}$ | C[a] $I_{obs}$ | C[a] $I_{der}$ |
|---|---|---|---|---|---|---|---|
| λ3727 [O II] | 0.257 | 32.7 | 122±46 | 55.8 | 221±35 | ... | |
| λ3869 [Ne III] | 0.231 | ... | | 48.7 | 165±37 | ... | |
| λ4340 Hγ | 0.135 | ... | | 31.0 | 63±10 | ... | |
| λ4363 [O III] | 0.129 | ... | | 17.3 | 34±9 | ... | |
| λ4686 He II | 0.043 | 100.5 | 129±17 | 64.6 | 84±6 | ... | |
| λ4740 [Ar IV] | 0.030 | ... | | 8.2 | 10.1±4 | ... | |
| λ4861 Hβ | 0.000 | 100.0 | 100 | 100.0 | 100 | ... | |
| λ4959 [O III] | -0.024 | 278.4 | 251±13 | 499.9 | 450±17 | ... | |
| λ5007 [O III] | -0.030 | 917.8 | 788±40 | 1590.4 | 1357±50 | ... | |
| λ5200 [N I] | -0.083 | ... | | 28.1 | 18.4±1.7 | ... | |
| λ5412 He II | -0.133 | 20.4 | 11.1±3.0 | ... | | ... | |
| λ5755 [N II] | -0.205 | ... | | 66.1 | 21.7±1.1 | ... | |
| λ5876 He I | -0.225 | ... | | 34.2 | 10.1±0.7 | ... | |
| λ6300 [O I] | -0.298 | ... | | 112.9 | 23.1±1.0 | ... | |
| λ6312 [S III]+He II | -0.299 | 33.2 | 7.3±0.8 | 46.4 | 9.5±0.6 | ... | |
| λ6364 [O I] | -0.310 | ... | | 39.8 | 7.7±0.4 | ... | |
| λ6436 [Ar V] | -0.316 | 32.9 | 6.5±0.8 | 7.7 | 1.4±0.3 | ... | |
| λ6548 [N II] | -0.338 | 159.7 | 28.5±2.6 | 1795.5 | 297±11 | 254.9 | 255±23 |
| λ6563 Hα | -0.340 | 1417.3 | 253±18 | 1788.5 | 295±11 | 100.0 | 100 |
| λ6584 [N II] | -0.343 | 686.8 | 123±6.2 | 6384.7 | 1055±39 | 1119.8 | 1120±97 |
| λ6678 He I | -0.353 | ... | | 15.5 | 2.4±0.3 | ... | |
| λ6717 [S II] | -0.362 | 47.3 | 7.6±0.5 | 395.2 | 59±2.2 | ... | |
| λ6731 [S II] | -0.364 | 56.3 | 9.1±0.6 | 467.4 | 69±2.6 | ... | |
| λ7005 [Ar V] | -0.380 | 99.5 | 13.8±0.9 | 30.0 | 4.0±0.3 | ... | |
| λ7135 [Ar III] | -0.396 | 173.4 | 21.7±1.2 | 327.1 | 40±1.5 | ... | |
| F(Hβ)[b] | | | 27.4 | | 150.4 | | ... |
| F(Hα)[b] | | | 69.4 | | 443.6 | | 2.76 |

[a] Intensities scaled to $I_{H\alpha} = 100.0$.

[b] Dereddened flux in units of $10^{-13}$ ergs cm$^{-2}$ s$^{-1}$.

TABLE 2

Plasma Diagnostics and Chemical Abundances

| | A | | B | |
|---|---|---|---|---|
| $T_e$ [N II] | 11075[a] | | 11075 | ±175 |
| $T_e$ [O III] | 11075[a] | | 16800 | ±2000 |
| $n_e$ [S II] | 1120 | ±280 | 1100 | $^{+25}_{-25}$ |
| $O^{++}/H^+ \times 10^5$ | 20.4 | ±2. | 11.5 | ±4. |
| $O^+/H^+ \times 10^5$ | 3.6 | ±2. | 6.0 | ±1.5 |
| $O^0/H^+ \times 10^5$ | ... | | 3.6 | ±0.4 |
| $O/H \times 10^4$ | 2.4 | | 2.8 | |
| $N^+/H^+ \times 10^5$ | 1.8 | ±0.2 | 17.1 | ±1.3 |
| $N/H \times 10^4$ | 1.24 | | 10.0 | |
| $S^+/H^+ \times 10^7$ | 3.6 | ±0.5 | 29.7 | ±2.4 |
| $S/H \times 10^6$ | 3.9 | | 26.0 | |
| $Ar^{++}/H^+ \times 10^7$ | 15.7 | ±1.4 | 13.5 | ±3. |
| $Ar^{3+}/H^+ \times 10^7$ | ... | | 11. | ±5. |
| $Ar^{4+}/H^+ \times 10^7$ | 23.7 | ±2. | 5.2 | ±0.9 |
| $Ar/H \times 10^6$ | 3.9 | | 3.0 | |
| $Ne^{++}/H^+ \times 10^5$ | ... | | 2.3 | ±1. |
| $Ne/H \times 10^5$ | ... | | 5.6 | |
| $He^+/H^+$ (5876) | ... | | 0.089 | ±0.012 |
| $He^{++}/H^+$ (4686) | 0.15 | ±0.03 | 0.090 | ±0.015 |
| He/H | ≥0.15 | | 0.18 | |
| $N^+/O^+$ | 0.5 | $^{+0.75}_{-0.21}$ | 2.85 | $^{+1.24}_{-0.75}$ |
| $N^+/S^+$ | 50 | | 57.6 | |

[a] Assumed values.

regarding collisional excitation (e.g., Clegg 1987). Given that the ionization potentials to produce $N^+$ and $O^+$ are similar, we set $N^+/O^+$ equal to N/O.

## 4. DISCUSSION

The electron density is almost the same in region A and in the outer shell zone B. This result would exclude a density enhancement due to a shock front between the inner region and the attached shell. In fact, shock excitation does not seem to play any significant role, as deduced from the low [O I] λ6300 to Hα ratio (Riera 1990). We can then conclude that the quasi-multiple shell structure is not due, in this case, to dynamical phenomena.

From Table 2 we see that the helium and nitrogen abundances are high. These results confirm the earlier work of Aller & Keyes (1987), who found N/O = 1.7 and He/H = 0.19 and subsequently classified M1-75 as a Type I PN. However, they did not carry out a spatially resolved abundance calculation. If we refer to region B, where the abundance determinations are very reliable, the N/O ratio (equal to 2.85) is among the highest ever found in a PNs. To be sure of this statement, we calculated the elemental abundances using our method, from the line fluxes given by other authors in the cases of the PNs (K3-61, M1-35, M1-42, and Me2-2) with very high abundances (Henry 1990; Perinotto 1991). We have referred to the original line flux determination (Aller & Keyes 1987), and found that in all four cases there was no possible determination of the electron temperature, whose value was assumed to be 10,000 K. Among the PNs with higher N/O we found, NGC 2440, Hu 1-2, M3-3, and, NGC 6302. Peimbert & Torres-Peimbert (1987) reported values of N/O equal to 1.5, 1.6 and 1.7 for NGC 2440, Hu 1-2 and M3-3, respectively. Aller et al. (1981) found a value of N/O = 1.6 for NGC 6302. All those values are far below the N/O ratio of M1-75.

Calculations by Becker & Iben (1980) and Garcia-Berro & Iben (1994) show that, after the second dredge-up, N/O abundances are lower or equal to unity. Iben & Tutukov (1995) predict that, for binary evolution in a common envelope phase, with initial mass between four and 6 solar masses, a nitrogen and helium enrichments very close to the ones observed by us in M1-75. However, there is no indication that M1-75 hosts a binary star, nor is any star observable; thus we cannot conclude that the object has gone through the necessary common envelope phase.

On the whole, the scenario including binarity of the nucleus is only an indication at this point, given the impossibility to observe the very faint central star. Further investigation on the central star of nebulae similar to M1-75 will certainly help to the understanding of the evolutionary path of their precursors.

The IAC80 is operated on the island of Tenerife by the Instituto de Astrofisica de Canarias in the Spanish Observatorio del Teide. The 2.5 m Isaac Newton Telescope is operated on the island of La Palma by the Royal Greenwich Observatory in the Spanish Observatorio del Roque de los Muchachos of the Instituto de Astrofísica de Canarias. This research was partially funded through grant PB90-0570 from the Dirección General de Investigación Científfica y Técnica of the Spanish Ministerio de Educación y Ciencia.

## REFERENCES

Aller, L. H., & Keyes, C. D. 1987, ApJS, 65, 405
Aller, L. H., Ross, J. E., O'Hara, B. J., & Keyes, C. D. 1981, MNRAS, 197, 95
Becker, S. A., & Iben, I., Jr. 1980, ApJ, 237, 111
Brocklehurst, M. 1971, MNRAS, 153, 471
Clegg, R. E. S. 1987, MNRAS, 229, 31p
Garcío-Berro, E., & Iben, I. 1994, ApJ, 434, 599
Henry, R. B. C. 1990, ApJ, 356, 229
Iben, I., & Tutukov, A. 1995, ApJ, preprint
Manchado, A., Guerrero, M. A., Stanghellini, L., & Serra-Ricart, M. 1995, in preparation
Peimbert, M. 1978, IAU Symp. 76, Planetary Nebulae, Observations and Theory, ed. Y. Terzian (Dordrecht: Reidel), 215
Peimbert, M., & Torres-Peimbert, S. 1987, Rev. Mexicano Astr. Af., 14, 540
Perinotto, M. 1991, ApJS, 76, 687
Preite-Martinez, A. 1986, private communication
Riera, A. 1990, Ph.D. thesis, Universidad de La Laguna
Schwarz, H. E., Corradi, R. L. M., & Melnick, J. 1992, A&AS, 96, 23
Stanghellini, L., Corradi, R. L. M., & Schwarz, W. M. 1978, A&A, 279, 521
Unger, S. W., Brinks, E., Laing, R. A., Tritton, K. P., & Gray, P. M. 1988, Observers' Guide, Version 2.0, Isaac Newton Group (La Palma), 101
Whitford, A. E. 1958, AJ, 63, 201